THE JOURNAL OF BIOLOGICAL CHEMISTRY VOL. 285, NO. 41, pp. 31418–31426, October 8, 2010

Zmynd15 Encodes a Histone Deacetylase-dependent Transcriptional Repressor Essential for Spermiogenesis and Male Fertility*[S]

Received for publication, February 21, 2010, and in revised form, July 29, 2010 Published, JBC Papers in Press, July 30, 2010, DOI 10.1074/jbc.M110.116418

Wei Yan[‡1], Yue Si[§], Sarah Slaymaker[§], Jiachen Li[‡], Huili Zheng[‡], David L. Young[‡], Ara Aslanian[§], Laura Saunders[¶], Eric Verdin[¶], and Israel F. Charo[§2]

From the [‡]Department of Physiology and Cell Biology, University of Nevada School of Medicine, Reno, Nevada 89557 and the [§]Gladstone Institute of Cardiovascular Disease and the [¶]Gladstone Institute of Virology and Immunology, San Francisco, California 94158

Spermatogenesis is a complex process through which male germ line stem cells undergo a multi-step differentiation program and sequentially become spermatogonia, spermatocytes, spermatids, and eventually spermatozoa. In this process, transcription factors act as switches that precisely regulate the expression of genes that in turn control the developmental program of male germ cells. Transcription factors identified to be essential for normal haploid gene expression all display transcription-activating effects and thus serve as the "on" switch for haploid gene expression. Here, we report that ZMYND15 acts as a histone deacetylase-dependent transcriptional repressor and controls normal temporal expression of haploid cell genes during spermiogenesis. Inactivation of *Zmynd15* results in early activation of transcription of numerous important haploid genes including *Prm1*, *Tnp1*, *Spem1*, and *Catpser3*; depletion of late spermatids; and male infertility. ZMYND15 represents the first transcriptional repressor identified to be essential for sperm production and male fertility.

Spermatogenesis is a process of cellular multiplication and differentiation through which male germ cells develop from spermatogonial stem cells to spermatozoa with highly specified functions (1, 2). Spermatogenesis can be divided into three phases: the mitotic phase (proliferation and differentiation of spermatogonia), the meiotic phase (differentiation of spermatocytes), and spermiogenesis (differentiation of haploid germ cells from round spermatids to elongated spermatids and spermatozoa) (1, 2). Within the seminiferous tubules, the developing male germ cells including spermatogonia, spermatocytes, and spermatids are all in close contact with the cytoplasm of supporting Sertoli cells, and these spermatogenic cells form specific cellular associations, which have been termed stages (3). For example, at stage VII, type A1 spermatogonia, preleptotene spermatocytes, step 7 round spermatids, and step 16 elongated spermatids are associated with each other, whereas type A3 spermatogonia, zygotene spermatocytes, meiotically dividing spermatocytes, and elongating step 12 spermatids are grouped together. Twelve stages (stages I–XII) can be identified in the mouse seminiferous tubules (3). Meiosis is unique to germ cells, and spermiogenesis is unique to male germ cell development. Unique processes often require unique genes and gene products to execute the functions. This may explain why ~10% of the entire protein-encoding genes are dedicated to the regulation of spermatogenesis, and spermiogenesis alone involves at least 500 testis-specific genes (4–6).

Another unique feature in the control of gene expression during spermiogenesis is the uncoupling of transcription and translation (7–12), which results from the fact that genes required for late spermiogenesis (step 9–16 spermatids in mice) have to be transcribed in round spermatids (steps 1–8) because transcription ceases when nuclear elongation and condensation start at step 9 of spermatid development in mice. Therefore, the most active transcription occurs at a time window between the late pachytene spermatocyte and round spermatid stages during spermatogenesis. The transcripts are then stabilized and stored until they are translated in later steps where their encoded proteins are needed (8, 9, 12).

Transcription factors are critical regulators of gene expression and serve as switches that control the normal spatiotemporal expression of gene sets during specific cellular processes (12). Given that so many testis-specific genes are involved in sperm production, the regulation of gene expression in spermatogenesis by testis-specific transcription factors is a foreseeable mechanism. Efforts in gene discovery in conjunction with gene knock-out technology over the past 15 years have identified a number of transcription factors that are preferentially or exclusively expressed in the testis and are required for different phases of male germ cell development (13–15). ZBTB16 (16, 17), SOX3 (18, 19), and SOHLH (20) are essential for the mitotic phase of spermatogenesis, and a lack of these transcription factors causes depletion of spermatogonia and eventually "Sertoli-only" testes. CREM-tau is essential for post-meiotic germ cell development, and a lack of this transcription factor leads to the arrest in the first step of spermiogenesis (21).

* This work was supported, in whole or in part, by National Institutes of Health Grants HL 52773 and HL 63894 (to I. F. C.) and HD 048855 and HD 05028 (to W. Y.). This work was also supported by National Institutes of Health Grant P20-RR-016464 (to the Nevada Genomic Center).

[S] The on-line version of this article (available at http://www.jbc.org) contains supplemental Tables S1 and S2 and Figs. S1–S4.

[1] To whom correspondence may be addressed: Dept. of Physiology and Cell Biology, University of Nevada School of Medicine, 1664 North Virginia St., MS352, Reno, NV 89557. Tel.: 775-784-7765; Fax: 775-784-6903; E-mail: wyan@medicine.nevada.edu.

[2] To whom correspondence may be addressed: Gladstone Institute of Cardiovascular Disease, 1650 Owens St., San Francisco, CA 94158. Tel.: 415-734-2000; Fax: 415-355-0960; E-mail: icharo@gladstone.ucsf.edu.

CREM-tau acts as a main switch for genes required for haploid germ cell development, including *Prm1*, *Prm2*, *Tnp1*, and *Tnp2* (21, 22). TBPL1 (TATA box-binding protein-like 1) is also required for spermiogenesis, and inactivation of *Tbpl1* results in a complete arrest of spermiogenesis at step 7 (23). Many genes that are under the control of TBPl1 fail to be expressed in the *Tbpl1*-null mice.

In the present study, we report that *Zmynd15* encodes a MYND-containing zinc-binding protein that is exclusively expressed in haploid germ cells during spermatogenesis. ZMYND15 acts as a transcription repressor through the recruitment of histone deacetylase enzymes (HDACs).[3] Inactivation of *Zmynd15* in mice results in late spermiogenic disruption, causing azoospermia and complete male infertility.

EXPERIMENTAL PROCEDURES

Zmynd15$^{-/-}$ *Mice*—We previously generated *Cxcl16*$^{-/-}$ mice in which the entire coding region and part of the 5′-untranslated region (UTR) of *Cxcl16* were deleted (24). We later discovered that *Zmynd15* and *Cxcl16* genes overlap in their 5′-UTRs (see Fig. 1*A*), and the deletion of the *Cxcl16* 5′-UTR in fact also inactivated *Zmynd15* (see Fig. 1*B*). The *Cxcl16*-null mice are actually *Cxcl16-Zmynd15* double knock-out mice (see "Results"). Because the testicular phenotype is caused by *Zmynd15* deficiency (see "Results" and "Discussion"), we henceforth call these mice *Zmynd15*$^{-/-}$ mice.

Testes Weight and Sperm Count—Whole testes were dissected and weighed. Spermatozoa were collected from caudal epididymides and incubated in 2 ml of PBS prewarmed to 37 °C. Sperm counts were performed using a hemocytometer (Hausser Scientific, Horsham, PA).

Generation of ZMYND15 Antibody—Keyhole limpet hemocyanin-conjugated peptide corresponding to amino acids 176–190 of murine ZMYND15 (PREDERAPEKRKGQKN) was synthesized and used for immunization of rabbits (Invitrogen). ELISA was used to quantify anti-ZMYND15 titers in serum, and the IgG fraction was then purified by chromatography on protein A columns (Pierce), following the manufacturer's protocol.

Histology and Immunohistochemistry—Wild-type and *Zmynd15*$^{-/-}$ testis were collected, fixed in 4% paraformaldehyde in PBS, and processed for sectioning. For histology the sections were deparaffinized in xylene, rehydrated by standard procedures, and stained with the Periodic acid-Schiff solution followed by hematoxylin counterstaining (25). Immunohistochemistry was performed as described (26), and anti-ZMYND15 antibodies were diluted at 1:600.

Quantitative and Semi-quantitative PCR—Whole testes were homogenized in TRIzol (Invitrogen), and total RNA was isolated following manufacturer's instructions. RNA samples were further purified using RNeasy mini columns (Qiagen) and then incubated with DNase (DNAfree, Ambion, Houston, TX) to eliminate potential genomic DNA contamination. For qPCR analyses, 1 μg of total RNA was reverse transcribed in a 20-μl reaction with SuperScript III Platinum Two-Step qRT-PCR kit (Invitrogen). The cDNA samples were diluted 10-fold, and 5 μl was added to a 50-μl PCR. To quantify *Zmynd15* expression, 2.5 μl of 20× predetermined TaqMan primer/probe sets from Applied Biosytems were used. The samples underwent the following protocol: stage 1, 50 °C for 2 min; stage 2, 95 °C for 10 min; and stage 3, 95 °C for 15 s, and followed by 60 °C for 1 min. Stage 3 was repeated 40 times. The relative expression levels were calculated by the comparative C_t method as outlined in the manufacturer's technical bulletin. Measured RNA levels were normalized to glyceraldehyde-3-phosphate dehydrogenase. Semi-qPCR analyses were performed as described (27). The cycle numbers were tested empirically to assure that the PCRs were within the exponential range. The primers and PCR conditions used in this study are listed in the supplemental Table S1.

In Situ Hybridization—*In situ* hybridization was performed as described (28, 29). Briefly, Bouin-fixed, paraffin-embedded adult mouse testes were cut into 5-μm sections, dewaxed, fixed, hybridized, and washed. A PCR-generated cDNA fragment (505 bp) corresponding to nucleotides 1–505 of the full-length *Zmynd15* cDNA was subcloned into the pGEM-T vector (Promega, Madison, WI). Sense and antisense riboprobes were generated and labeled with [α-^{35}S]UTP with a riboprobe labeling system (Promega, Madison, WI). Hybridization signals were detected by autoradiography with an NTB-2 emulsion (Eastman Kodak Co.). After development and fixation, the slides were counterstained with hematoxylin and mounted for photography.

TUNEL Assay—We performed TUNEL assays on paraformaldehyde-fixed paraffin sections using an ApoTag Plus peroxidase kit (Intergen, Purchase, NY) according to the manufacturer's instructions.

Transcription Repression Assay—10t1/2 cells were grown to 75–80% confluency in three six-well plates. All of the cells were transfected with 1 mg of total DNA and FuGENE 6 (Roche Applied Science) and with 200 ng of SV40-luc and 200 ng of CMV-lacZ. One six-well plate was transfected with 600 ng of Gal4-DBD, another plate with 300 ng of Gal4-DBD and 300 ng of Gal4-Zmynd15, and a final plate with 600 ng of Gal4-Zmynd15. After 24 h, half of each plate was treated with the HDAC inhibitor trichostatin A (Calbiochem, Gibbstown, NJ), and the other half of each plate was treated with dimethyl sulfoxide. After another 24 h, the cells were washed with 1× PBS, and the cell lysates were harvested with 250 ml of reporter lysis buffer (Promega). Luciferase activity was measured in 50 ml of sample lysates with a luciferase assay system (Promega). Transfection efficiency was normalized to β-galactosidase, which was measured in 50 ml of sample lysate by a β-galactosidase enzyme assay system (Promega). The experiments were performed in three replicates, and statistic significance was evaluated using the Student's *t* test (Sigma Stat).

Cell-based Pulldown Assays—Constructs for expressing FLAG-tagged histone deacetylases 1, 3, 5, 6, and 7 and SIRT1 were prepared as described previously (30–33). 293T cells were grown in DMEM (Mediatech, Herndon, VA) supplemented with 10% FBS (Gemini Bio-products, Woodland, CA), 1% penicillin-streptomycin, and 2 mM L-glutamine (Invitrogen). 1 ×

[3] The abbreviations used are: HDAC, histone deacetylase enzyme; UTR, untranslated region; qPCR, quantitative PCR; Mes, 4-morpholineethanesulfonic acid; P*n*, postnatal day *n*.

10^6 293T cells were plated per 100 mM dish, 24 h before calcium-phosphate transfection. A total of 20 μg of DNA (10 μg of pCDNA HDAC C-terminal FLAG tag + 10 μg of ZMYND15 HA tag) was brought up to 876 μl in H_2O. 124 μl of 2 M $CaCl_2$ was added to the DNA, 1 ml of 2× HEPES-buffered saline (0.01 M HEPES, 0.14 M NaCl, 0.01% NaN_3), pH 7.05, was bubbled in for 10 s, and then the mixture was applied to the cells. 48 h after transfection the cells were washed with 1× PBS and lysed directly in the 100 mm plate in 333 μl of cold lysis buffer (50 mM Tris-HCl, pH 7.5, 0.5 mM EDTA, 500 mM NaCl, 0.5% Nonidet P-40, and 1× complete protease inhibitors (Roche Applied Science) for 1 h and then diluted with 666 μl of lysis buffer with no NaCl to get a final concentration of 150 mM NaCl. The cell lysates were cleared by centrifuged for 15 min at 14,000 × *g*, and 0.01% of the lysate was analyzed to check for expression of transfected proteins. 40 μl of prewashed M2 agarose beads (catalog number A2220; Sigma-Aldrich) were added to the lysates to immunoprecipitate the FLAG-tagged HDACs, and the lysates were rotated at 4 °C for 2–16 h. The beads were collected by centrifugation for 30 s at 5,000 × *g*, and the supernatants were removed by aspiration. The pellets were washed five times with 0.5 ml of lysis buffer. 75 μl of 2× sample buffer was added to the M2 agarose beads, the samples were boiled for 3 min, and the immunoprecipitated proteins were analyzed by SDS-PAGE and immunoblotted using anti-ZYMND15 antibody and a rabbit anti-FLAG antibody (catalog number F7425; Sigma).

Microarray Analyses—Total RNAs were isolated from *Zmynd15*$^{-/-}$ and wild-type testes at P20. Duplicates for each genotype were subjected to microarray analyses. Affymetrix mouse genome 430A 2.0 microarrays (Affymetrix Inc., Santa Clara, CA) were hybridized at the Nevada Genomic Center. In brief, 5 μg of total RNA was converted to first strand cDNA by using Superscript II reverse transcriptase primed by a poly(T) oligomer that incorporated the T7 promoter. Second strand cDNA synthesis was followed by *in vitro* transcription for linear amplification of each transcript and incorporation of biotinylated CTP and UTP. The cRNA products were fragmented to 200 nucleotides or less, heated at 99 °C for 5 min, and hybridized for 16 h at 45 °C to MOE430A microarrays. The microarrays were then washed at low (6× 0.18 M NaCl, 10 mM phosphate, pH 7.4, 1 mM EDTA) and high (100 mM Mes, 0.1 M NaCl) stringency and stained with streptavidin-phycoerythrin. Fluorescence was amplified by adding biotinylated anti-streptavidin and an additional aliquot of streptavidin-phycoerythrin stain. A confocal scanner was used to collect fluorescence signal at 3-μm resolution after excitation at 570 nm. Affymetrix gcos 1.2 software was used to analyze and quantify the hybridized arrays. The Affymetrix mas5 algorithm (with default settings, as encoded in gcos 1.2) was used to generate signal values and to determine present/absent/marginal flags for each probe set on each array. Probe sets flagged by mas5 as present are described as detected.

Analysis of Microarray Data—Analysis was performed using Bioconductor, a publicly available group of software packages as described (34). Briefly, the packages used included Simpleaffy, Limma, Annaffy, and GOstats. Simpleaffy was used to preprocess individual probe intensities from CEL files into expression values from which fold changes were derived using Limma. Robust multiple-array analysis, which uses quantile normalization for cross-chip normalization, was used to preprocess the data. The main advantage of quantile normalization is that it controls outliers while not significantly reducing sensitivity. The significance of differential expression was determined using an empirical Bayes approach (Limma) for controlling the standard error of intensity of each probe set based on the standard errors of the intensities of all other probe sets in the comparison. After *p* values were obtained for each gene, they were adjusted using the Benjamini-Hochberg method (34). This method converts *p* values, which are measures of the false positive rate, into *Q* values, which are measures of false discovery rate. The Benjamini-Hochberg method allows a more direct control of false results while not reducing sensitivity as much as other methods for *p* value adjustment. Annaffy was used to annotate each gene probe set and to tabulate information such as GenBank™ accession numbers, chromosome locations, and gene ontology terms.

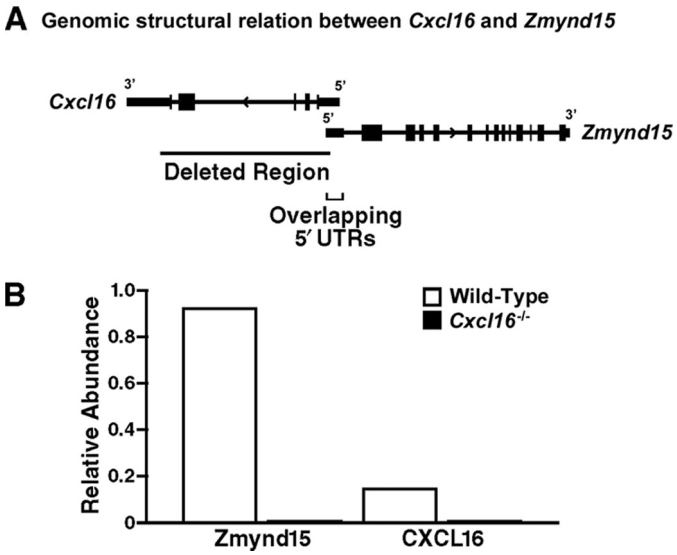

FIGURE 1. **Inadvertent co-inactivation of *Cxcl16* and *Zmynd15* in mice.** *A*, genomic structural relation between *Cxcl16* and *Zmynd15*. *Cxcl16* and *Zmynd15* are in opposite orientations with overlapping 5′-UTRs, and our targeting strategy deleted the 5′-UTRs for both genes. *B*, qPCR analyses of levels of *Cxcl16* and *Zmynd15* mRNAs in wild-type and *Cxcl16*-null testes.

RESULTS

Deletion of the 5′-UTR of Cxcl16 Resulted in Inactivation of Zmynd15—In our earlier studies designed to investigate the role of scavenger receptors in cardiovascular diseases, we generated *Cxcl16* knock-out mice by deleting the 5′-UTR and the entire coding region of *Cxcl16* using homologous recombination in murine embryonic stem cells (24). Surprisingly, we found that all *Cxcl16*$^{-/-}$ males were infertile. We expected no fertility problems in *Cxcl16*-null male mice because levels of *Cxcl16* mRNA in the testis were very low compared with other organs (*e.g.* heart and kidney), and mRNA for CXCR6, the only known receptor for CXCL16, was not detected in the testis. Furthermore, male and female *Cxcr6*$^{-/-}$ mice are completely fertile (35). By re-examining the targeting site flanking *Cxcl16*, we found that in fact *Cxcl16* and *Zmynd15* are adjacent to each other on chromosome 11 and possess overlapping 5′-UTRs (Fig. 1*A*). Our targeting vector deleted all of the *Cxcl16* coding

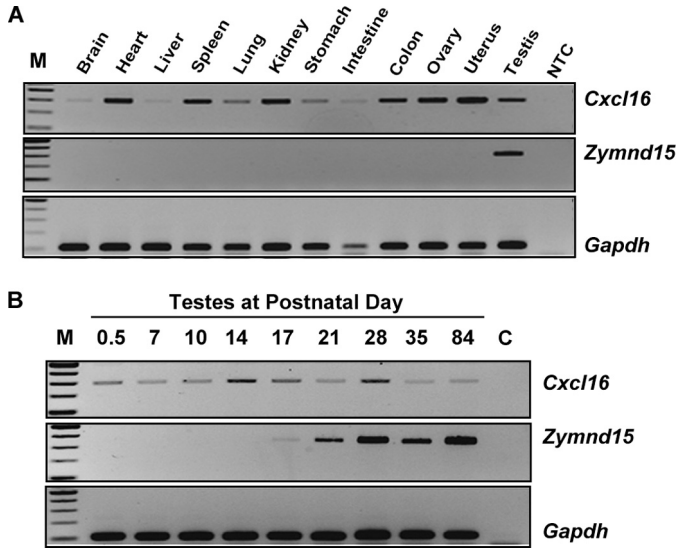

FIGURE 2. **Expression profiles of *Cxcl16* and *Zymnd15* mRNAs in mice.** *A*, RT-PCR analyses of levels of *Cxcl16* and *Zymnd15* mRNAs in 12 organs of adult mice. *Lane M*, 100-bp molecular marker. *NTC*, nontemplate control. *Gapdh* was used as a loading control. *B*, RT-PCR analyses of *Cxcl16* and *Zymnd15* mRNA expression in developing testes. *Lane M*, 100-bp molecular marker; *Lane C*, nontemplate control. *Gapdh* was used as a loading control.

exons and most of the 5′-UTR, which is shared by *Zmynd15*. It was thus highly likely that the *Cxcl16* targeting vector also inadvertently disrupted the *Zmynd15* promoter. Our qPCR analyses on levels of *Cxcl16* and *Zmynd15* mRNAs in wild-type and *Cxcl16*$^{-/-}$ testes confirmed that in our previously thought *Cxcl16*-null testes, both *Cxcl16* and *Zmynd15* were totally inactivated (Fig. 1*B*). In addition, in WT testes levels of *Zmynd15*, mRNAs were ~10 times greater than those of *Cxcl16*.

Zmynd15 Is a Testis-specific Gene Highly Expressed in Spermiogenesis—We examined the expression of *Zmynd15* in 12 adult mouse organs and also in developing testes using RT-PCR (Fig. 2). Unlike *Cxcl16*, which was expressed in a ubiquitous manner, *Zmynd15* was exclusively detected in the testis (Fig. 2*A*). We also searched the Genehub-GEPIS database (36, 37) for *Zmynd15* and found that expressed sequence tags for human *ZMYND15* were exclusively derived from the testis. In developing testes, *Cxcl16* was detected in all ages with comparable levels (Fig. 2*B*). In contrast, *Zmynd15* was first detected on postnatal day 17 (P17), and its levels increase at P21 and thereafter (Fig. 2*B*), suggesting that *Zmynd15* mRNA started to be expressed in late pachytene spermatocytes and later in spermatids. Moreover, our data are consistent with previous microarray data on *Zmynd15* expression in purified spermatogenic cells and developing testes in the Gene Expression Omnibus database, showing that *Zmynd15* is expressed in pachytene spermatocytes and round spermatids (Gene Expression Omnibus profile GDS2390), the onset of *Zmynd15* expression is at P18, and its levels increase thereafter and peak in adult testes (Gene Expression Omnibus profile GDS606).

Zmynd15 encodes a protein of 703 amino acids in mice that contains a zinc finger MYND motif and a nuclear localization sequence (supplemental Fig. S1). Alignment analyses revealed that ZMYND15 is highly conserved among mice,

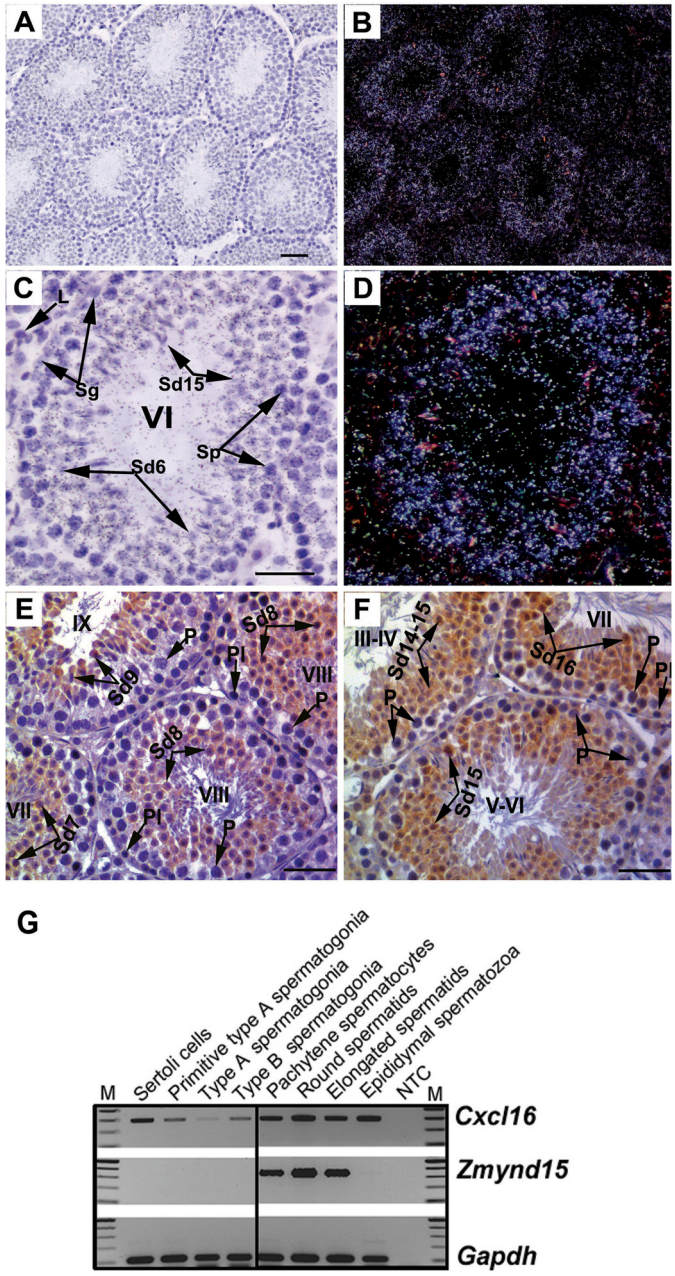

FIGURE 3. **Localization of *Zmynd15* mRNA and protein in the mouse testis.** *A–D*, *in situ* hybridization analyses of *Zmynd15* mRNA localization in the testis of adult mice. Bright (*A* and *C*) and corresponding dark (*B* and *D*) field images are shown. The lower magnification images (*A* and *B*) show that the hybridization signals (*black dots* in bright field images and *silver grains* in dark field images) are confined to the luminal and adluminal compartments, and the higher power images (*C* and *D*) reveal that the hybridization signals are over pachytene spermatocytes and spermatids. The *arabic numbers* stand for steps of spermatid development, and the *Roman numerals* indicate stages of the seminiferous epithelial cycles. *Sg*, spermatogonia; *Sp*, spermatocytes; *Sd*, spermatids; *L*, Leydig cells. *Scale bars*, 20 μm. *E* and *F*, ZMYND15 immunoreactivity is detected mainly in the nuclei of step 2–8 round spermatids (*E* and *F*). In step 9–11 spermatids, ZMYND15 immunoreactivity appears to shift to cytoplasm (*E*). The *arabic numbers* stand for steps of spermatid development, and *Roman numerals* indicate stages of the seminiferous epithelial cycles. *P*, pachytene spermatocytes; *Pl*, preleptotene spermatocytes; *Sd*, spermatids. *Scale bars*, 20 μm. *G*, RT-PCR analyses of expression of *Cxcl16* and *Zmynd15* mRNAs in purified testicular cell types. *Lane M*, 100-bp molecular marker. *NTC*, nontemplate control.

rats, and humans (supplemental Fig. S1), as evidenced by >85% homology in their amino acid sequences.

To further determine the cellular origin of *Zmynd15* expression, we performed *in situ* hybridization and immunohistochemistry to localize *Zymnd15* mRNA and protein in the testis (Fig. 3). Hybridization signals (represented by silver grains in dark field images) were detected in pachytene spermatocytes and all developing spermatids (steps 1–16) (Fig. 3, *A–D*). No signals were observed in either Sertoli cells or Leydig cells. The hybridization signals were first detected in early pachytene spermatocytes, and the intensity of the hybridization signals were higher in step 1–13 spermatids than in pachytene spermatocytes and late spermatids at steps 14–16. *Zmynd15*-null testis sections were used as a negative control, and no hybridization signals were detected (data not shown). Our *in situ* hybridization data are consistent with the RT-PCR data on developing testes (Fig. 2*B*), demonstrating that *Zmynd15* mRNA is expressed predominantly in pachytene spermatocytes and spermatids.

To determine *Zmynd15* protein localization, we next performed immunohistochemistry on wild-type adult mouse testis sections using a polyclonal anti-ZMYND15 antibody. Immunoreactivity was first detected in step 2 round spermatids (Fig. 3, *E* and *F*). The intensity of the staining continuously increased thereafter and peaked in spermatids at steps 7–9. ZMYND15 levels started to decrease after step 9, and interestingly, in step 9–11 elongating spermatids, ZMYND15 immunoreactivity appeared to shift from the nucleus to the cytoplasm. No specific staining was detected when *Zmynd15*$^{-/-}$ testis sections were used (data not shown). Semi-quantitative PCR analyses using cDNAs prepared from purified testicular cell populations further confirmed that unlike *Cxcl16*, which was ubiquitously expressed in virtually all cell types within the testis, *Zmynd15* mRNA was mainly expressed in pachytene spermatocytes and spermatids (Fig. 3*G*). Taken together, these data demonstrate that *Zmynd15* is exclusively expressed in the testis and is localized to the developing haploid germ cells in the testis. A schematic summary of the localization patterns of *Zmynd15* mRNA and protein during spermatogenesis is presented in supplemental Fig. S2.

Inactivation of Zmynd15 Causes Spermiogenic Disruption, Azoospermia, and Male Infertility in Mice—Despite the fact that the *Cxcl16* knock-out mice are in fact *Cxcl16-Zmynd15* double knock-outs, their spermatogenic defects are likely caused by the inactivation of *Zmynd15* based upon the abundant testis-specific expression and consistency between the late spermiogenic defects and the expression sites and function of ZMYND15 (see below). We initially observed that when male *Zmynd15*$^{-/-}$ male mice were mated with wild-type female mice for >6 months, no litters were born. Further timed mating experiments revealed that 10 of 10 wild-type female mice that were mated with *Zmynd15*$^{+/-}$ male mice (as judged by the presence of vaginal plugs next morning after adding the females to the male cages) became pregnant and later produced 10 litters with normal litter size (~6–8 pups in the C57Bl/6: 129Sv/Ev hybrid background), whereas none of the 10 wild-type females that were mated with *Zmynd15*$^{-/-}$ males were pregnant and produced any litters. *Zmynd15*$^{-/-}$ females, on the other hand, displayed normal fertility. *Zmynd15*-null testes showed ~25% reduction in weight (Fig. 4*A*).

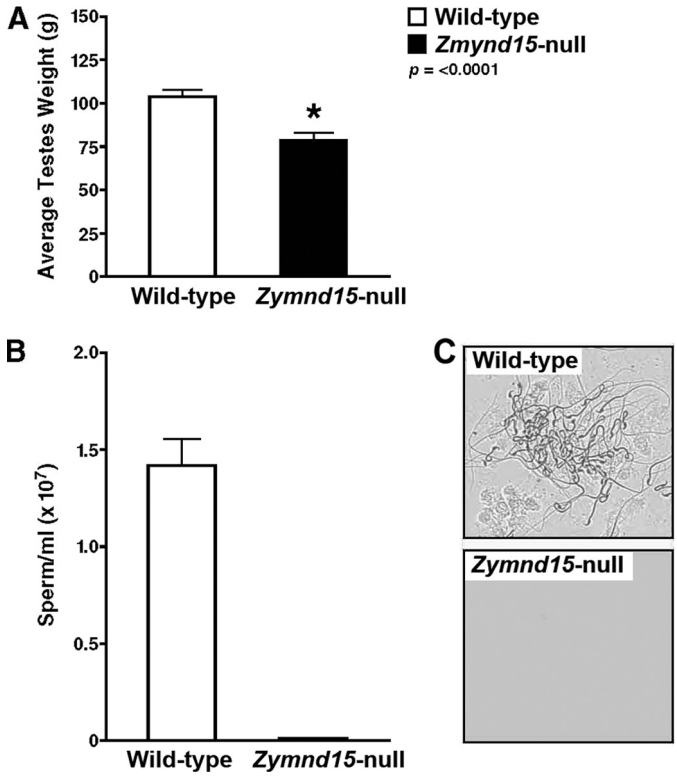

FIGURE 4. **Zmynd15-null male mice display reduced testis weight and azoospermia.** *A*, *Zmynd15*-null testes display ~25% reduction in weight. *B*, epididymal sperm counts in wild-type and *Zmynd15*-null male mice. *C*, numerous spermatozoa were collected from the cauda epididymis of wild-type mice (*upper panel*), whereas no spermatozoa were found in the cauda epididymis of *Zmynd15*-null mice (*lower panel*).

No spermatozoa were found in the caudal epididymis (Fig. 4*B*) of *Zmynd15*-null mice. Reduced testicular weight and the lack of spermatozoa in the epididymis suggest a spermatogenic disruption in the *Zmynd15*-null testes. Histological examination of the *Zmynd15*-null testes revealed a severe depletion of haploid spermatids characterized by spermatids detaching from the seminiferous epithelium and sloughing into the lumen of the seminiferous tubules (Fig. 5, *A–D*). Most of the seminiferous tubules in the *Zmynd15*-null testes lacked or a showed reduced number of late haploid cells (elongating and elongated spermatids). It was difficult to stage each cross-section of the *Zmynd15*-null seminiferous tubules because of the severe spermatid depletion, but the tubules displayed less severely disrupted histology and were mainly at stages IX–XII. We thus estimated that those tubules with severe spermatid depletion were mainly stage I–VIII tubules (for criteria of the mouse seminiferous epithelium staging see Ref. 3 and supplemental Fig. S2). Round spermatids were still present in the majority of the stage I–VIII tubules, and thus it appeared that the depleted haploid cells were mainly step 13–16 elongated spermatids. Closer examination of the seminiferous tubules indicated that few, if any, step 13–16 spermatids were present, and in stage I–VIII tubules where elongated spermatids were actively depleted, round spermatids appeared to be being depleted as well, although they were still present

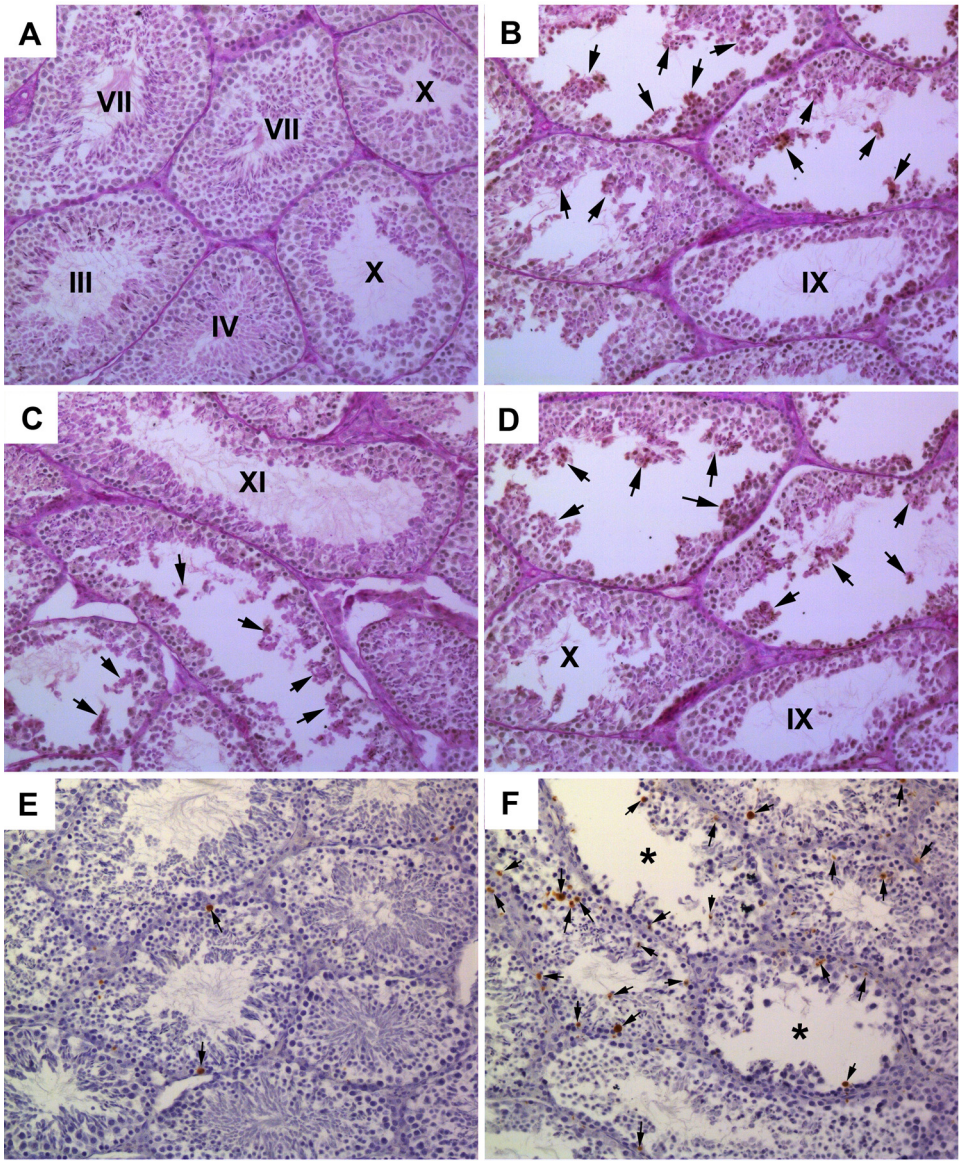

FIGURE 5. **Spermatogenic disruption in the testes of *Zmynd15*$^{-/-}$ mice.** *A–D*, wild-type testes display robust spermatogenesis (*A*), whereas *Zmynd15*$^{-/-}$ testes showed severe spermatid depletion characterized by spermatid clusters that are detaching from the seminiferous epithelium followed by sloughing into the lumen of the seminiferous tubules (*arrows* in *B–D*). The *Roman numerals* indicate stages of the seminiferous epithelial cycles. *A–D* are in the same magnification. *Scale bar*, 20 μm. *E* and *F*, TUNEL analyses of cell apoptosis showed very few apoptotic germ cells in wild-type testes (*E*), whereas in *Zmynd15*-null testes many TUNEL-positive germ cells resembling mainly round spermatids and spermatocytes are present (*F*). *E* and *F* are in the same magnification. *Scale bar*, 20 μm.

(supplemental Fig. S3). Consistent with the depletion of both elongated and round spermatids in the *Zmynd15*-null testes, numerous pycnotic-looking cells resembling round spermatids were observed in the epididymis (supplemental Fig. S4). The depletion of spermatids appeared to be achieved via detaching from the epithelium followed by sloughing into the lumen. The depleted haploid cells mostly existed as clusters of multiple cells, probably because they were all interconnected by intercellular bridges (Fig. 5, *A–D*). TUNEL assays demonstrated that spermatids that appeared to be depleted were TUNEL-negative, suggesting that apoptosis is not the mechanism underlying the depletion of defective late spermatids (Fig. 5, *E* and *F*). A lack of apoptosis in late spermatids has been well documented in numerous previous studies (38). However, it is noteworthy that the number of TUNEL-positive germ cells resembling mainly spermatocytes was increased in the tubules with severe spermatid depletion (Fig. 5, *E* and *F*). Given that the majority of spermatocytes were present and appeared normal, it is likely that this enhanced spermatocyte apoptosis was secondary to the primary spermatid defects that disrupted the microenvironment of the seminiferous tubules or communications between spermatocytes and spermatids.

The normal size of the accessory sex organs including the seminal vesicle and normal histology of the Leydig cells in the testis suggest that the testosterone levels were normal in the *Zmynd15*-null males. Indeed, we measured both FSH and luteinizing hormone levels and found no significant differences between wild-type and *Zmynd15*-null males (data not shown). Taken together, these data demonstrate that inactivation of *Zmynd15* gene causes severe depletion of late spermatids (steps 13–16), characterized by detaching from the seminiferous epithelium followed by sloughing into the lumen of the seminiferous tubules. *Zmynd15*-null males thus display azoospermia and complete male infertility.

Function of ZMYND15 as a Transcriptional Repressor through Interaction with HDACs—ZMYND15 belongs to a family of MYND domain-containing zinc finger proteins (Fig. 3) that are commonly involved in transcriptional repression through interacting with histone deacetylases in chromatin remodeling (39, 40). We therefore performed a transcriptional repression assay to determine whether ZMYND15 also acted as such a repressor. ZMYND15 fused to Gal-4 inhibited SV40-driven luciferase expression in a dose-dependent manner in 10t1/2 cells (Fig. 6*A*). The HDAC inhibitor trichostatin A (41, 42) was then used to determine whether the ZMYND15-mediated repression of transcription was HDAC-dependent. An addition of trichostatin A (150 μM) significantly inhibited the GAL4-ZMYND15 repression (Fig. 6*A*). Similar results were obtained when COS-1 cells were used (data not shown). These results suggest that the effects of ZMYND15 on the luciferase expression are mediated, at least in part, through recruitment of HDACs.

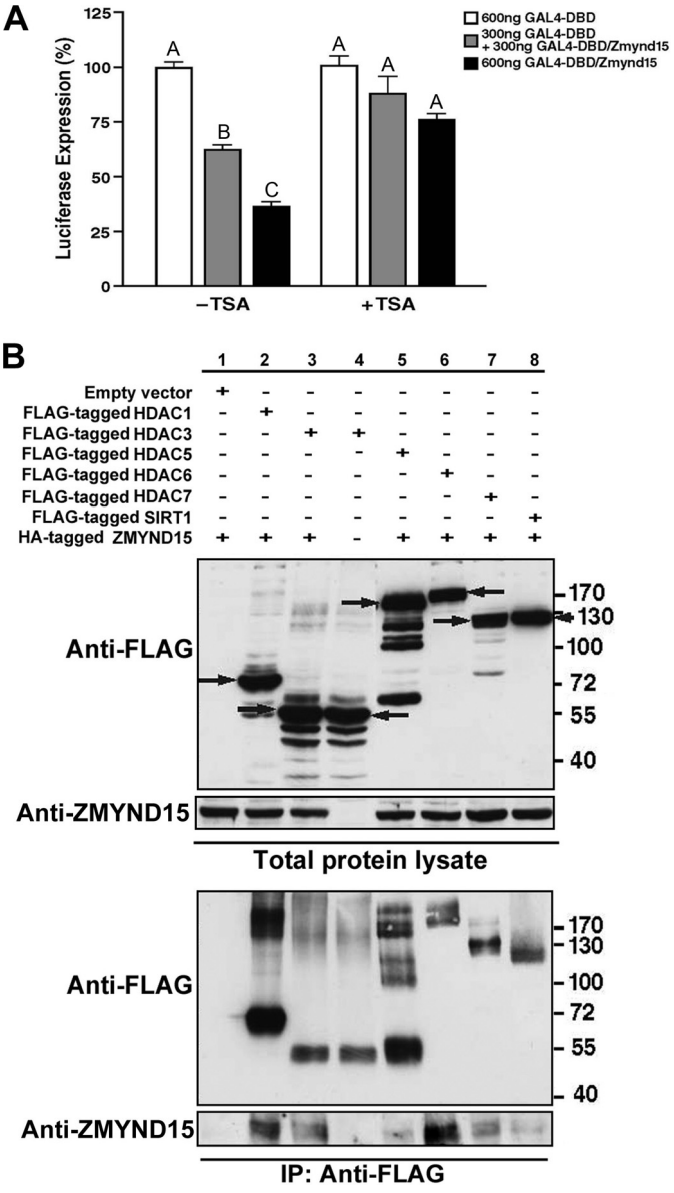

FIGURE 6. **ZMYND15 acts as a HDAC-dependent transcription repressor.** *A*, 10T1/2 cells were transfected with GAL4-DBD or GAL4-DBD/ZMYND15 along with 5XGAL4-SV40-luc as indicated. The HDAC inhibitor trichostatin A (*TSA*, 150 nM) was added 24 h after transfection. Transfection efficiency was normalized to β-galactosidase. The results shown represent the averages of three replicates (means ± S.E.). The response for GAL4-DBD alone is set at 100%. The *bars* labeled with different letters are significantly different ($n = 3$, $p < 0.01$). *B*, ZMYND15 co-immunoprecipitates with Class I and IIb HDACs. Protein extracts from 293T cells co-transfected with C-terminal FLAG-tagged HDACs (empty vector (*lane 1*), HDAC1 (*lane 2*), HDAC3 (*lanes 3* and *4*) HDAC5 (*lane 5*), HDAC6 (*lane 6*), HDAC7 (*lane 7*), or SIRT1 (*lane 8*)) and HA-tagged ZMYND15 (*lanes 1–3* and *5–8*) were analyzed by Western blot using anti-FLAG or anti-ZYMND15 antisera to demonstrate protein expression (*upper two panels* of *B*). The *lower two panels* show the co-immunoprecipitation of FLAG-tagged HDACs with HA-tagged ZMYND15. *IP*, immunoprecipitation.

We then performed pulldown (cotransfection followed by immunoprecipitation) assays to test the potential direct physical interactions between ZMYND15 and HDACs (Fig. 6*B*). We first verified the expression of all transfected expression vectors in 293T cells (Fig. 6*B*, *upper two panels*). We then used anti-FLAG to pull down different HDAC complexes and detected the presence or absence of ZMYND15 using anti-HA antibody (Fig. 6*B*). ZMYND15 was co-immunoprecipitated with

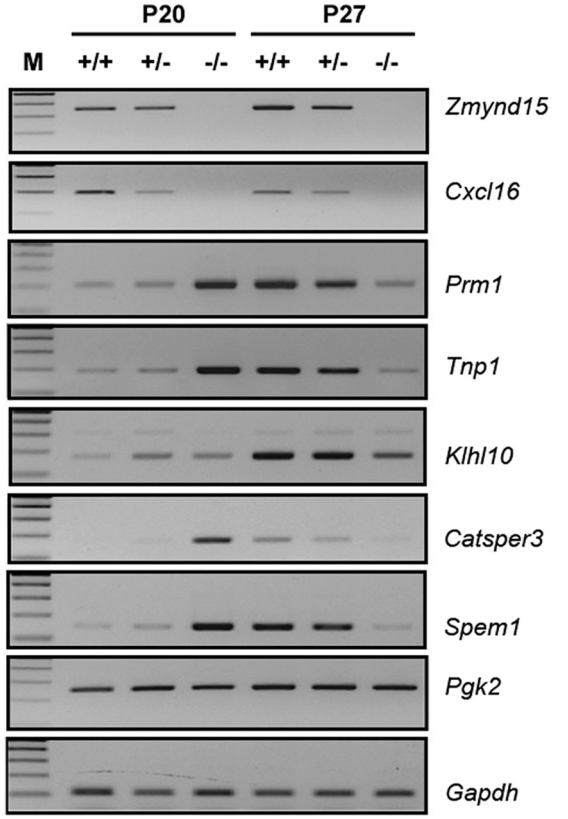

FIGURE 7. **Selective deregulation of haploid gene expression.** Semi-qPCR analyses were used to determine mRNA levels of five spermatid-specific genes (*Prm1*, *Tnp1*, *Klhl10*, *Catsper3*, and *Spem1*) in the wild-type and *Zmynd15*$^{-/-}$ testes. mRNAs for the five haploid genes are barely detectable in the wild-type testes at P20 because the onset of their transcription is in early round spermatids (steps 1–5). Four (*Prm1*, *Tnp1*, *Catsper3*, and *Spem1*) of the five spermatid-specific genes examined are drastically elevated in the *Zmynd15*$^{-/-}$ testes at P20. At P27, mRNA levels of the five haploid genes are much higher than those in *Zmynd15*$^{-/-}$ testes most likely because of the ongoing depletion of spermatids in the absence of ZMYND15. The images represent one of the three independent experiments using three sets of mice with different genotypes. *Lane M*, 100-bp molecular marker. *Gapdh* was used as a loading control.

HDAC1, HDAC3, and HDAC6 and to a lesser extent with HDAC7, indicating that it indeed binds both Class I and II HDACs (Fig. 6*B*). Little or no binding to HDAC5 or the Class III HDAC SIRT1 was detected.

Deregulation of Transcription of Haploid Genes—Given that ZMYND15 interacted with HDACs and acted as a transcription repressor, we further examined the expression of five well characterized haploid genes known to be essential for normal spermiogenesis and male fertility, including *Prm1* (43), *Tnp1* (44), *Klhl10* (45), *Catsper3* (46, 47), and *Spem1* (26) during testicular development in wild-type, heterozygous, and *Zmynd15*-null male mice (Fig. 7). Round spermatids first appear in the seminiferous epithelium at ~P20, and at P27 spermatids have developed to step 13 or 15 (48). Previous studies have shown that these five genes begin to be transcribed in round spermatids between steps 1 and 6 and that levels increase gradually thereafter and peak in step 8–12 spermatids (26, 27, 43, 45, 46, 49). Consistent with the transcription onset in round spermatids, in wild-type P20 testes, levels of mRNAs for *Prm1*, *Tnp1*, *Catsper3*, and *Spem1* were barely detectable, whereas in *Zmynd15*-null testes, the levels of the four mRNAs were dras-

tically increased. At p27, the levels of the four haploid mRNAs increased in the wild-type testes but decreased in the *Zmynd15*-null testes because of the onset of spermatid depletion (Fig. 7). *Klhl10* is another haploid gene, and its levels remained unchanged at P20 and down-regulated at P27 because of spermatid depletion in the *Zmynd15*$^{-/-}$ testes compared with in wild-type testes. This suggests that *Zmynd15* selectively represses transcription of a subset of haploid genes. *Pgk2* is mainly expressed in pachytene spermatocytes (50, 51), and its mRNA levels remained unchanged, suggesting that the defects were mainly confined to the early haploid phase (round spermatids). The depletion of step 13–16 spermatids observed is thus a delayed reflection of the primary defects in haploid gene expression that occur in early round spermatids.

To further determine global changes in testicular mRNA transcriptome in the absence of *Zmynd15*, we conducted gene chip analyses using the Affymetrix mouse genome 430A 2.0 microarrays. P20 was chosen as the time point for transcriptome comparison because no morphologically discernable disruptions have occurred at this point, and thus the cellular composition between the *Zmynd15*-null and WT testes remains the same. The microarray data showed that among ~20,000 unique probe sets analyzed, 341 genes displayed more than 2-fold increases in mRNA levels in the *Zmynd15*-null testes at P20, whereas only 18 genes showed more than 2-fold of decreases in their mRNA levels (supplemental Table S2). The remaining testicular mRNAs showed no or less than 2-fold changes in their levels. The microarray data are consistent with our qPCR data on five spermiogenesis-specific genes, showing significantly increased levels of *Prm1*, *Tnp1*, *Catpser3*, and *Spem1* mRNAs and similar levels of *Klhl10* and *Pgk2* mRNAs in *Zmynd15*-null testes compared with WT testes at P20 (highlighted in *yellow* in supplemental Table S2). The absence of both *Cxcl16* and *Zmynd15* in the gene chip analyses of *Zmynd15*-null testis samples further demonstrates the validity of the microarray data. We then compared the 341 up-regulated genes in the P20 *Zmynd15*-null testes (supplemental Table S2) with a list of 348 testis-specific genes that are mainly expressed in haploid male germ cells (spermatids)[4] and found that 53 of the 341 up-regulated genes are spermatid-specific ones (highlighted in *green* in supplemental Table S2). The lack of a repressor does not necessarily lead to accumulation of mRNAs. Nevertheless, these data do further support a role for ZMYND15 acting as a transcription repressor to regulate spatiotemporal expression of a large subset of haploid genes.

DISCUSSION

Although both *Cxcl16* and *Zmynd15* are inactivated in the mouse line analyzed in this study, it is highly likely that the spermiogenic disruption is caused by *Zmynd15* inactivation. Several lines of evidence support this claim. First, the only known receptor for CXCL16 is CXCR6, which is not expressed in the testes (35). Moreover, both male and female *Cxcr6*$^{-/-}$ mice are fertile (35). Second, *Cxcl16* is expressed in essentially all testicular cell types including Sertoli cells, Leydig cells, spermatogonia, spermatocytes, and spermatids at low levels (Fig. 3*G*). In contrast, ZMYND15 is exclusively expressed in spermatids, implying a specific role in spermatids. The primary defects in these male mice are confined to spermatids, which coincides with the expression site of ZMYND15. Third, abnormal spatiotemporal transcription of numerous haploid genes is consistent with a role in transcriptional regulation of ZMYND15 because it functions as a repressor of transcription by interacting with HDACs. Therefore, we believe that it is the *Zmynd15* deficiency that causes the disruption in haploid gene expression and consequently the late spermatid depletion and male infertility.

Transcription is very active in the late meiotic and early haploid phases because many genes required for late spermiogenesis have to be transcribed before transcription ceases because of nuclear condensation and elongation from step 9 onward (7–12). CREM-tau has been shown to act as a main transcription activator for the expression of many haploid genes including *Prm1*, *Prm2*, *Tnp1*, and *Tnp2* (21, 22). ZMYND15 is, to our knowledge, the first spermatid-specific transcription repressor identified to date. This notion is supported by the transcription repression assays *in vitro* and the enhanced transcription of numerous haploid genes in the absence of ZMYND15. This finding is of significance because it indicates that the haploid gene transcription not only requires transcriptional activators but also needs transcription repressors, and the balance between the transcriptional activation and repression is essential for normal spatiotemporal haploid gene expression. *Zmynd15* thus represents the first transcription repressor identified to be essential for normal spatiotemporal expression of haploid genes.

Human ZMYND15 shares a high degree of sequence homology with mouse ZMYND15 (~85%) and is also exclusively expressed in the testis, suggesting that they have similar physiological roles. The necessity of ZMYND15 in the regulation of normal spatiotemporal expression of critical haploid genes in mice implies that similar azoospermia phenotype would occur in humans if the human *ZMYND15* gene is disrupted by mutations. Therefore, it would be informative to screen the nonobstructive azoospermia patients for potential *ZMYND15* mutations.

Like many of the MYND domain-containing zinc finger proteins, ZMYND15 selectively binds Class I and II HDACs and can suppress transcription in a HDAC-dependent manner in our *in vitro* assays. Future direct immunoprecipitation assays using testis protein lysates and reporter assays using promoters of ZMYND15 target genes will further corroborate these findings under more physiological conditions. In addition, the downstream events after ZMYND15 binding to different members of HDACs need to be determined in future studies. Microarray analyses identified numerous haploid transcripts that are up-regulated in the absence of ZMYND15. Moreover, the number of up-regulated transcripts is much greater than that of down-regulated transcripts (241 up-regulated *versus* 18 down-regulated). These data are supportive of a transcriptional suppressive role of ZMYND15. However, these up-regulated transcripts may not necessarily be the target genes of ZMYND15, because many of these up-regulated transcripts may reflect secondary effects caused by the absence of ZMYND15. Therefore, future transcriptional suppression

[4] Y. Zhang, Z. Zheng, J. Li, and W. Yan, unpublished data.

assays using promoters of these up-regulated transcripts will enable us to determine the true target genes of ZMYND15.

In summary, we have discovered that ZMYND15, a previously uncharacterized MYND domain-containing zinc finger protein, interacts with histone deacetylases and acts as a testis-specific transcriptional repressor that plays an essential role in the regulation of spatiotemporal expression of many haploid genes. Because transcription factors are key regulators of gene expression, identification of novel transcription factors essential for spermatogenesis enables us to not only reveal the gene network utilized in male germ cell development but also provide mechanistic insights for the identification of novel causative genes of male infertility and future development of male nonhormonal contraceptives.

REFERENCES

1. Fawcett, D. W. (1975) *Dev. Biol.* **44,** 394–436
2. Oakberg, E. F. (1956) *Am. J. Anat.* **99,** 391–413
3. Ahmed, E. A., and de Rooij, D. G. (2009) *Methods Mol. Biol.* **558,** 263–277
4. Lin, Y. N., and Matzuk, M. M. (2005) *Semin. Reprod. Med.* **23,** 201–212
5. Schultz, N., Hamra, F. K., and Garbers, D. L. (2003) *Proc. Natl. Acad. Sci. U.S.A.* **100,** 12201–12206
6. Shima, J. E., McLean, D. J., McCarrey, J. R., and Griswold, M. D. (2004) *Biol. Reprod.* **71,** 319–330
7. Eddy, E. M. (1998) *Semin. Cell Dev. Biol.* **9,** 451–457
8. Eddy, E. M. (2002) *Recent Prog. Horm. Res.* **57,** 103–128
9. Hecht, N. B. (1988) *Prog. Clin. Biol. Res.* **267,** 291–313
10. Hecht, N. B. (1990) *J. Reprod. Fertil.* **88,** 679–693
11. Sassone-Corsi, P. (1998) *Semin. Cell Dev. Biol.* **9,** 475–482
12. Sassone-Corsi, P. (2002) *Science* **296,** 2176–2178
13. Maclean, J. A., 2nd, and Wilkinson, M. F. (2005) *Curr. Top Dev. Biol.* **71,** 131–197
14. Matzuk, M. M., and Lamb, D. J. (2002) *Nat. Cell Biol.* **4,** (suppl.) S41–S49
15. Matzuk, M. M., and Lamb, D. J. (2008) *Nat. Med.* **14,** 1197–1213
16. Buaas, F. W., Kirsh, A. L., Sharma, M., McLean, D. J., Morris, J. L., Griswold, M. D., de Rooij, D. G., and Braun, R. E. (2004) *Nat. Genet.* **36,** 647–652
17. Costoya, J. A., Hobbs, R. M., Barna, M., Cattoretti, G., Manova, K., Sukhwani, M., Orwig, K. E., Wolgemuth, D. J., and Pandolfi, P. P. (2004) *Nat. Genet.* **36,** 653–659
18. Raverot, G., Weiss, J., Park, S. Y., Hurley, L., and Jameson, J. L. (2005) *Dev. Biol.* **283,** 215–225
19. Weiss, J., Meeks, J. J., Hurley, L., Raverot, G., Frassetto, A., and Jameson, J. L. (2003) *Mol. Cell. Biol.* **23,** 8084–8091
20. Ballow, D., Meistrich, M. L., Matzuk, M., and Rajkovic, A. (2006) *Dev. Biol.* **294,** 161–167
21. Blendy, J. A., Kaestner, K. H., Weinbauer, G. F., Nieschlag, E., and Schütz, G. (1996) *Nature* **380,** 162–165
22. Nantel, F., Monaco, L., Foulkes, N. S., Masquilier, D., LeMeur, M., Henriksén, K., Dierich, A., Parvinen, M., and Sassone-Corsi, P. (1996) *Nature* **380,** 159–162
23. Martianov, I., Fimia, G. M., Dierich, A., Parvinen, M., Sassone-Corsi, P., and Davidson, I. (2001) *Mol. Cell* **7,** 509–515
24. Aslanian, A. M., and Charo, I. F. (2006) *Circulation* **114,** 583–590
25. Lähdetie, J. (1986) *Mutat. Res.* **172,** 255–263
26. Zheng, H., Stratton, C. J., Morozumi, K., Jin, J., Yanagimachi, R., and Yan, W. (2007) *Proc. Natl. Acad. Sci. U.S.A.* **104,** 6852–6857
27. Jin, J. L., O'Doherty, A. M., Wang, S., Zheng, H., Sanders, K. M., and Yan, W. (2005) *Biol. Reprod.*
28. Wu, M. H., Rajkovic, A., Burns, K. H., Yan, W., Lin, Y. N., and Matzuk, M. M. (2003) *Gene Expr. Patterns* **3,** 231–236
29. Yan, W., Hirvonen-Santti, S. J., Palvimo, J. J., Toppari, J., and Jänne, O. A. (2002) *Mech. Dev.* **118,** 247–253
30. Emiliani, S., Fischle, W., Van Lint, C., Al-Abed, Y., and Verdin, E. (1998) *Proc. Natl. Acad. Sci. U.S.A.* **95,** 2795–2800
31. Fischle, W., Dequiedt, F., Fillion, M., Hendzel, M. J., Voelter, W., and Verdin, E. (2001) *J. Biol. Chem.* **276,** 35826–35835
32. Fischle, W., Emiliani, S., Hendzel, M. J., Nagase, T., Nomura, N., Voelter, W., and Verdin, E. (1999) *J. Biol. Chem.* **274,** 11713–11720
33. North, B. J., Marshall, B. L., Borra, M. T., Denu, J. M., and Verdin, E. (2003) *Mol. Cell* **11,** 437–444
34. Chen, H., Ordög, T., Chen, J., Young, D. L., Bardsley, M. R., Redelman, D., Ward, S. M., and Sanders, K. M. (2007) *Physiol. Genomics* **31,** 492–509
35. Unutmaz, D., Xiang, W., Sunshine, M. J., Campbell, J., Butcher, E., and Littman, D. R. (2000) *J. Immunol.* **165,** 3284–3292
36. Zhang, Y., Eberhard, D. A., Frantz, G. D., Dowd, P., Wu, T. D., Zhou, Y., Watanabe, C., Luoh, S. M., Polakis, P., Hillan, K. J., Wood, W. I., and Zhang, Z. (2004) *Bioinformatics* **20,** 2390–2398
37. Zhang, Y., Luoh, S. M., Hon, L. S., Baertsch, R., Wood, W. I., and Zhang, Z. (2007) *Nucleic Acids Res.* **35,** W152–W158
38. Yan, W. (2009) *Mol. Cell. Endocrinol.* **306,** 24–32
39. Brown, M. A., Sims, R. J., 3rd, Gottlieb, P. D., and Tucker, P. W. (2006) *Mol. Cancer* **5,** 26
40. Gottlieb, P. D., Pierce, S. A., Sims, R. J., Yamagishi, H., Weihe, E. K., Harriss, J. V., Maika, S. D., Kuziel, W. A., King, H. L., Olson, E. N., Nakagawa, O., and Srivastava, D. (2002) *Nat. Genet.* **31,** 25–32
41. Pinnoji, R. C., Bedadala, G. R., George, B., Holland, T. C., Hill, J. M., and Hsia, S. C. (2007) *Virol. J.* **4,** 56
42. Zhang, Y., Liao, M., and Dufau, M. L. (2006) *Mol. Cell. Biol.* **26,** 6748–6761
43. Cho, C., Willis, W. D., Goulding, E. H., Jung-Ha, H., Choi, Y. C., Hecht, N. B., and Eddy, E. M. (2001) *Nat. Genet.* **28,** 82–86
44. Yu, Y. E., Zhang, Y., Unni, E., Shirley, C. R., Deng, J. M., Russell, L. D., Weil, M. M., Behringer, R. R., and Meistrich, M. L. (2000) *Proc. Natl. Acad. Sci. U.S.A.* **97,** 4683–4688
45. Yan, W., Ma, L., Burns, K. H., and Matzuk, M. M. (2004) *Proc. Natl. Acad. Sci. U.S.A.* **101,** 7793–7798
46. Jin, J., Jin, N., Zheng, H., Ro, S., Tafolla, D., Sanders, K. M., and Yan, W. (2007) *Biol. Reprod.* **77,** 37–44
47. Qi, H., Moran, M. M., Navarro, B., Chong, J. A., Krapivinsky, G., Krapivinsky, L., Kirichok, Y., Ramsey, I. S., Quill, T. A., and Clapham, D. E. (2007) *Proc. Natl. Acad. Sci. U.S.A.* **104,** 1219–1223
48. Bellvé, A. R. (1993) *Methods Enzymol.* **225,** 84–113
49. Zhao, M., Shirley, C. R., Hayashi, S., Marcon, L., Mohapatra, B., Suganuma, R., Behringer, R. R., Boissonneault, G., Yanagimachi, R., and Meistrich, M. L. (2004) *Genesis* **38,** 200–213
50. Robinson, M. O., McCarrey, J. R., and Simon, M. I. (1989) *Proc. Natl. Acad. Sci. U.S.A.* **86,** 8437–8441
51. Zhang, L. P., Stroud, J., Eddy, C. A., Walter, C. A., and McCarrey, J. R. (1999) *Biol. Reprod.* **60,** 1329–1337